Cell-Penetrating Peptide–Bismuth Bicycles

Saan Voss,[a,b] Liam D. Adair,[c,d] Katharina Achazi,[e] Heeyoung Kim,[f,g] Silke Bergemann,[b] Ralf Bartenschlager,[f,g] Elizabeth J. New,[c,d] Jörg Rademann,[b] and Christoph Nitsche*[a]

[a] Saan Voss, Assoc. Prof. Christoph Nitsche
Research School of Chemistry
Australian National University
Canberra, ACT 2601 Australia
E-mail: christoph.nitsche@anu.edu.au

[b] Saan Voss, Silke Bergemann, Prof. Dr. Jörg Rademann
Department of Biology, Chemistry and Pharmacy, Institute of Pharmacy, Medicinal Chemistry
Freie Universität Berlin
Königin-Luise-Str. 2+4, 14195 Berlin, Germany

[c] Dr. Liam D. Adair, Prof. Elizabeth J. New
School of Chemistry
The University of Sydney
Sydney, NSW 2006 Australia

[d] Dr. Liam D. Adair, Prof. Elizabeth J. New
Australian Research Council Centre of Excellence for Innovations in Peptide and Protein Science
The University of Sydney
Sydney, NSW 2006 Australia

[e] Dr. Katharina Achazi
Institut für Chemie und Biochemie
Freie Universität Berlin
Altensteinstraße 23a, 14195 Berlin, Germany

[f] Dr. Heeyoung Kim, Prof. Dr. Ralf Bartenschlager
Heidelberg University, Medical Faculty Heidelberg
Department of Infectious Diseases, Molecular Virology
Center for Integrative Infectious Diseases Research (CIID)
Heidelberg, Germany

[g] Dr. Heeyoung Kim, Prof. Dr. Ralf Bartenschlager
German Center for Infection Research, Heidelberg partner site
Heidelberg, Germany

Supporting information for this article is given via a link at the end of the document.

Abstract: Cell-penetrating peptides (CPPs) play a significant role in the delivery of cargos into human cells for a wide range of therapeutic and diagnostic applications. We disclose the first CPPs based on peptide–bismuth bicycles, which can be readily obtained from commercially available peptide precursors, making them highly accessible for a wide range of applications. These CPPs enter mammalian cells with high efficiency as demonstrated by live-cell microscopy using fluorescently labelled peptides. We report highly efficient sequences that demonstrate comparable cellular uptake to conventional CPPs, despite requiring only three positive charges. Bicyclization triggered by the presence of bismuth(III) increases cellular uptake by more than one order of magnitude. Through the analysis of cell lysates using inductive coupled plasma mass spectrometry (ICP-MS), we have introduced an alternative approach to examine the cellular uptake of CPPs without the use of fluorescent dyes. This has allowed us to confirm the presence of bismuth in cells after exposure to our CPPs.

Cell-penetrating peptides (CPPs) hold great promise as agents to facilitate the delivery of cargos, including drugs, nucleic acids, and probes, across mammalian cell membranes.[1] CPPs were used to deliver potent polymers and nanoparticles to drug targets localized in subcellular organelles. While mechanistic details are still debated, the majority of CPPs enter cells via endocytosis. Although recent reports have described uncharged sequences,[2] most CPPs are either polycationic or amphipathic. Noncanonical modifications, such as D-amino acids, unnatural side chains and macrocyclization are known to improve cellular uptake and overall stability.[3]

Constrained bicyclic peptides have emerged as valuable resources in biomedical research, offering antibody-like affinity, exceptional specificity, and superior metabolic stability;[4] however, the exploration of bicyclic peptides as CPPs remains limited.[5] Recently, we introduced peptide–bismuth bicycles as a novel class of bioactive peptides that possess structural constraints and can be synthesized under biocompatible conditions.[6] In this study, we present the first cell-penetrating bicyclic peptides that can be readily synthesized without the need for any noncanonical modifications. Our peptide–bismuth bicycles demonstrate efficient cellular uptake at low nanomolar concentrations, requiring only a small number of charged residues.

Peptide–bismuth bicycles are accessible via addition of Bi(III) salts to peptides containing three cysteine residues in physiological buffer.[6] In this study, we have enhanced our synthetic protocol by introducing a final ion exchange step as an

alternative to laborious HPLC purification (Scheme S2). This enables simultaneous bench-top purification of multiple bicyclic peptides, significantly enhancing the accessibility and availability of this compound class. To facilitate the analysis of cellular uptake through fluorescence microscopy, we incorporated rhodamine B (RhB) at the N-terminus of the peptide using solid-phase peptide synthesis (Scheme S1). In order to prevent spirolactam formation, we introduced a piperazine-succinate linker between the peptide and the RhB dye.[7] Based on these considerations, we synthesised our cationic model peptide **1** comprising two lysine and one arginine residues (KRK) in each cycle (Figure 1a).

Competition with thiol-containing compounds may influence the binding of the three peptide thiols to bismuth. To ascertain the integrity of the peptide in the reducing environment within cells, we evaluated its stability in the presence of glutathione (GSH), the predominant intracellular thiol. We used derivative **12**, which is structurally identical to compound **1** but lacks the dye and linker. Over the course of two days, we did not detect any degradation of **12** in the presence of up to 20 equivalents (2 mM) of GSH (Figure S1). Only at 100 equivalents (10 mM) of GSH we observed 30% degradation after two days (Figure S1). Given that the GSH concentration in most cells is about 1–2 mM (except for hepatocytes),[8] we conclude that the bismuth-cysteine bond is sufficiently stable to degradation by common intracellular thiols.

Encouraged by these results, we conducted flow cytometry experiments utilizing fluorescence-activated cell sorting (FACS) to examine the cellular uptake of compound **1** in MDA, HeLa, and HT-29 human cell lines. We performed measurements using a concentration gradient ranging from 0.1 to 10 µM (Figure 1c) and incubation times spanning from 0.5 to 4 h (Figure 1d). Both data sets demonstrate cellular uptake of **1** at sub-micromolar concentrations in all cell lines. Based on fluorescence intensity, the cellular uptake of **1** reaches its maximum between 4 and 12 h of incubation (Figure S34). Live-cell confocal microscopy studies with HeLa cells confirmed time-dependent uptake of **1** at 1 µM (Figure 1e). Control experiments using Lyso Tracker (LysoTracker™ Green DND-26 from Thermo Fisher Scientific), a fluorescent dye specific for acidic cell compartments, indicated partial colocalization of compound **1** in endo-lysosomes (Figure 1e, panel C). Cell nuclei (stained with Hoechst) remained free of **1**. Concentration-dependent subsequent microscopy experiments demonstrate that bicycle **1** exhibits cellular uptake even at concentrations as low as 10 nM (Figure S6).

Our subsequent objective was to explore alternative peptide sequences and compare our KRK motif with CPPs that have been reported in the literature (Table 1). In order to monitor the cellular uptake, compounds **1**-**11** were all modified with the identical RhB dye at the N-terminus and assessed in concentration- and time-dependent experiments by live-cell confocal microscopy (Figures S6 – S24) and FACS (Figures S25 – S57).

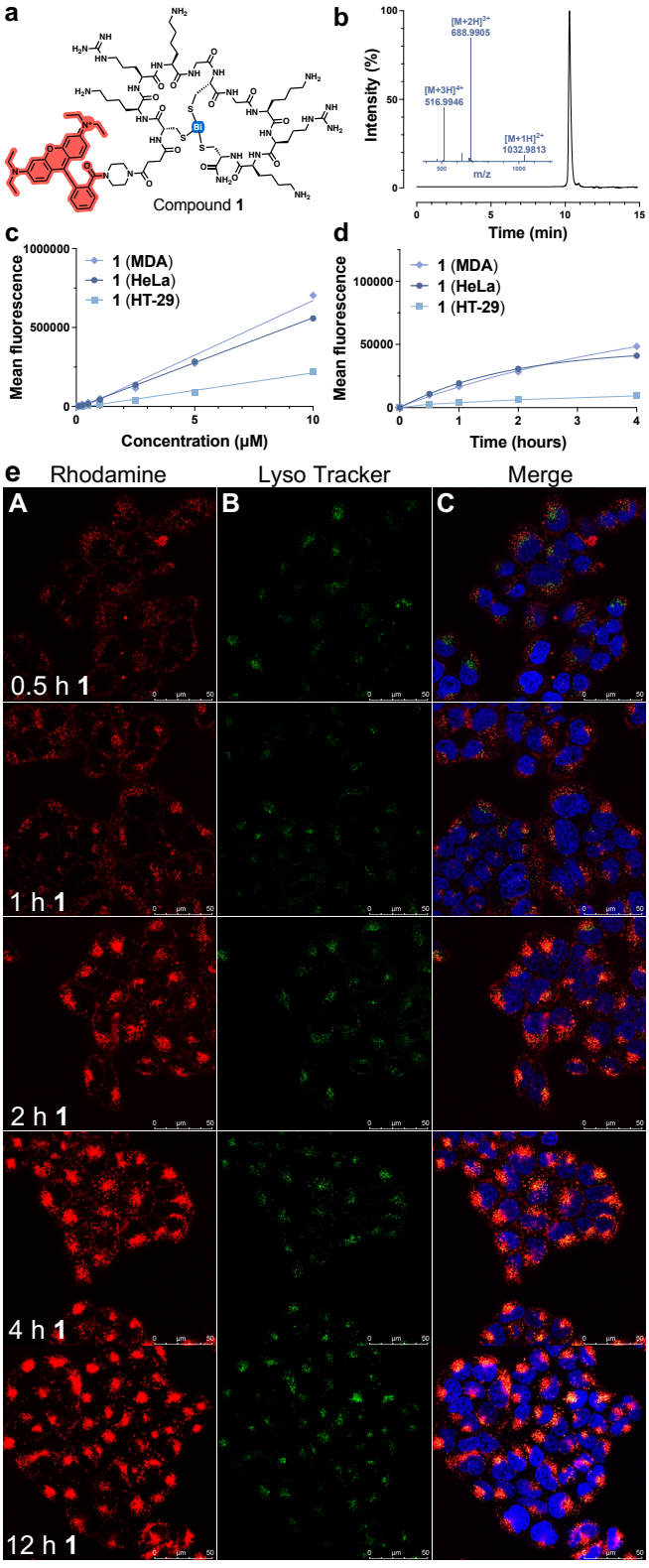

Figure 1. a) Structure of **1**. b) Chromatogram (254 nm) and MS spectrum of **1**. c) Concentration-dependent cellular uptake of **1** in HeLa, MDA and HT-29 cells (12 h incubation time) measured by flow cytometry. d) Time-dependent cellular uptake of **1** (1 µM) in HeLa, MDA and HT-29 cells measured by flow cytometry. e) Live-cell confocal microscopy images of HeLa cells treated with **1** (1 µM). Incubation times are indicated. Panel **A,** rhodamine fluorophore channel; panel **B,** Lyso Tracker channel; panel **C,** merged image of rhodamine, Lyso Tracker and Hoechst (nucleus stain) channels. Yellow colour indicates colocalization of rhodamine and Lyso Tracker in acidic compartments such as endosomes.

Table 1. Investigated peptides and their relative cellular uptake.

Cpd.	Sequence[a]	Relative uptake in HeLa cells[b]	
		FACS[c]	ICP-MS[d]
1	RhB-CKRKGCGKRKC	1.0	1.0
2	RhB-CSGSGCFΦRRRRC	1.1	0.3
3	RhB-SKRKGSFΦRRRRS	<0.1	
4	RhB-CKRKGCFΦRRRRC	2.7	
5	RhB-SFΦRRRRSGKRKS	<0.1	
6	RhB-CFΦRRRRCGKRKC	2.5	0.4
7	RhB-CKRKGCfΦRrRrC	2.7	0.4
8	RhB-CFWRRRRCFWRRRRC	3.0	0.5
9	RhB-CGWWGCfΦRrRrC	2.6	0.4
10	RhB-CGWWWGCfΦRrRrC	2.1	0.5
11	RhB-CGWfWGCfΦRrRrC	2.8	0.6
12	Ac-CKRKGCGKRKC		1.0
13	Ac-CFΦRRRRCGKRKC		1.1
14	Ac-CKRKGCrRrGrKkRrC		0.9
15	Ac-CSGSGCGKRKC		1.9
16	Ac-CKRKGCGSGSC		2.6
17	Bz-CROKORCROKORC		1.1
18	Bz-CKRKGCGROKORC		1.1
19	Bz-CKRKGCGROKORGC		1.4

[a] All peptides are bicyclic and contain Bi(III) bound to three cysteines except for linear control compounds **3** and **5**. All peptides contain a C-terminal amide. Small letters indicate D-amino acids. RhB, rhodamine B with piperazine linker; Φ, L-3-(2-naphtyl)alanine. [b] Cellular uptake relative to bicyclic peptide **1** after 4 h of incubation at 1 μM peptide concentration. [c] Relative uptake determined by fluorescence-activated cell sorting (FACS). [d] Relative uptake determined by inductively coupled plasma mass spectrometry (ICP-MS).

We analyzed various combinations of reported CPPs, our own sequence (KRK) and an uncharged control sequence (SGSG). Cyclic FΦRRRR (Φ, L-3-(2-naphtyl)alanine) and fΦrRrR (with alternating L- and D-amino acids), which were both reported by Pei and coworkers,[9] displayed increased cellular uptake when combined with KRK in bicycles **4**, **6**, and **7**. We further examined hydrophobic tryptophan-rich sequences (**9**-**11**) known for their potential to enhance endosomal escape;[10] however, we found no significant effects, which was corroborated by counterstaining with Lyso Tracker (Figures S14–S16, S21, S22, S24). This observation may be attributed to the high constraint of our bicyclic peptides compared to previous applications of these endosomal escape sequences in fusion proteins.

In order to prove that the peptide–bismuth bicycles enter the cells fully intact, as opposed to degradation before or during cell entry, we performed inductively coupled plasma mass spectrometry (ICP-MS) with HeLa cell lysates after 4 h of incubation with peptide–bismuth bicycles at 1 μM (Table 1). Cells were washed thoroughly prior lysis to remove any excess CPP. The bismuth amount was measured via ICP-MS, while the total protein concentration in lysates was determined from a bicinchoninic acid (BCA) assay. In the lysates of all analyzed peptides, we consistently observed the presence of bismuth, with typical concentrations ranging from 10 to 100 ng (0.05 – 0.5 nmol) bismuth per mg protein (Figure S3).

Leveraging the distinctive characteristics of cell-penetrating peptide–bismuth bicycles for ICP-MS analysis, we investigated bicyclic peptides without a fluorophore (**12**-**19**) and compared them to those containing the RhB fluorophore (**1**-**2**, **6**-**11**). On average, the peptides without fluorophore exhibited enhanced cellular uptake compared to those incorporating the RhB dye (Figure S3), suggesting that RhB has a slightly negative effect on the cellular uptake of cell-penetrating peptide–bismuth bicycles. However, the magnitude of this effect is relatively small, allowing hydrophobic cargos such as RhB to be successfully delivered into cells even at low nanomolar concentrations. This highlights the advantage of bismuth as a heavy atom label over fluorophore-labelling, as it avoids potential alterations to the properties of bioactive compounds.

We further examined the effects of varying positive charges on cellular uptake. Bicycles with ten or more positive charges, like **14** and **17**, showed similar levels of uptake compared to model compound **12** with six charges (Table 1). Compound **14** contains the previously reported cyclic TAT sequence with alternating L- and D-amino acids.[11] Bicycles that exhibited a substantial reduction in overall charge, with only one KRK motif present in either the N-terminal (**16**) or C-terminal cycle (**15**), demonstrated a twofold increase in cellular uptake (Table 1). Peptide **16** displayed the highest overall uptake with recovery of more than 100 ng bismuth per mg protein from HeLa cell lysates (Figure S3).

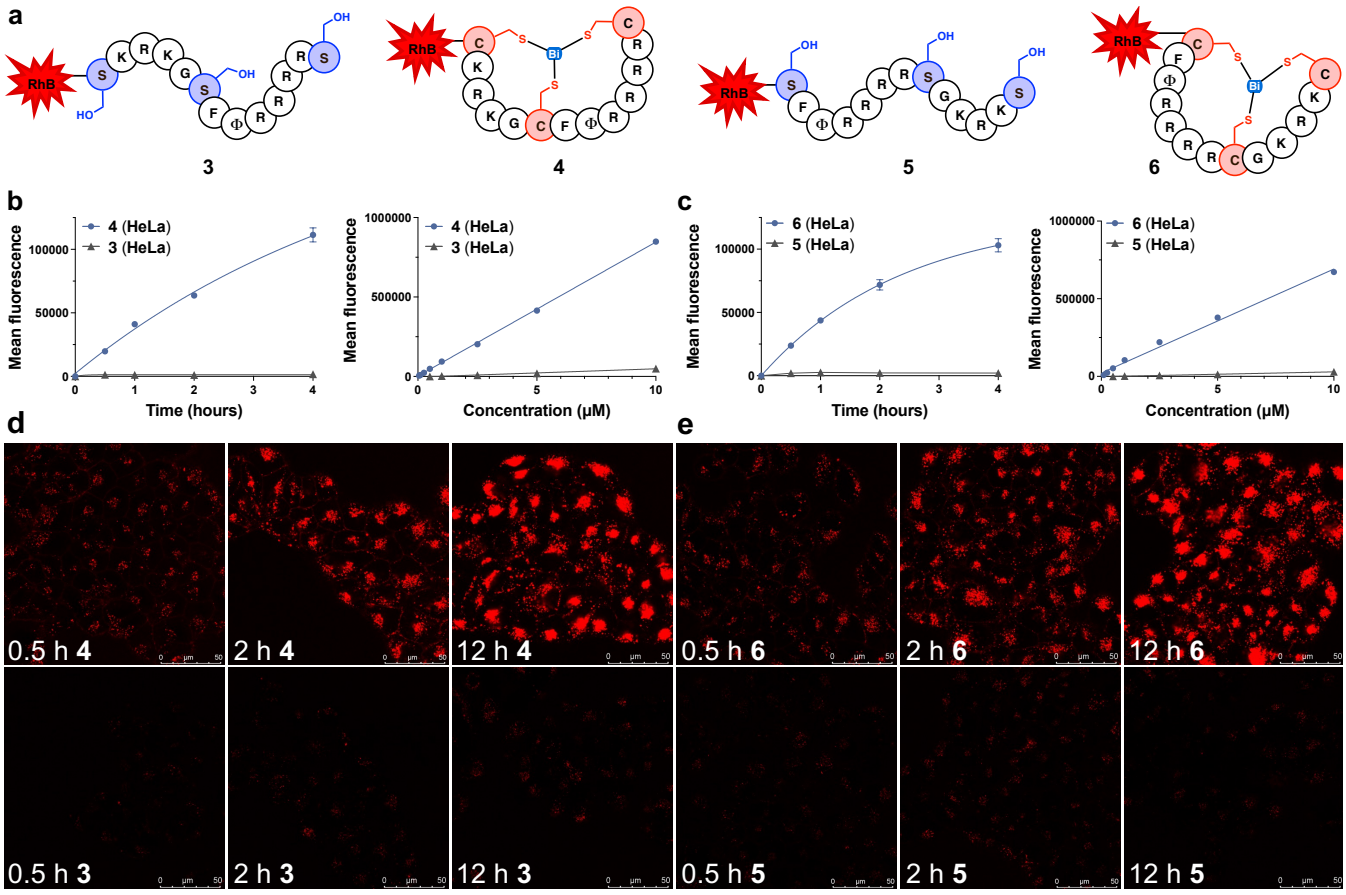

Figure 2. Comparison of cellular uptake in HeLa cells of fluorescently labelled linear peptides **3** and **5** and their corresponding peptide–bismuth bicycles **5** and **6**. a) Schematic structures of linear and bicyclic peptides. Φ, L-3-(2-naphtyl)alanine; RhB, rhodamine B with piperazine linker. Uptake of peptides **3** vs. **4** (b) and **5** vs. **6** (c) determined by flow cytometry as functions of time and concentration in HeLa cells. Time dependent uptake of peptides **3** vs. **4** (d) and **5** vs. **6** (e) at 1 μM determined by live-cell confocal microscopy. The rhodamine fluorophore channel is shown. Micrographs taken at additional time points and counter stains with Hoechst and Lyso Tracker are shown in the Supporting Information.

One advantage of utilizing bismuth in peptide bicycles is its significantly lower toxicity compared to other heavy metals that bind to cysteine residues.[12] However, a system that effectively delivers bismuth into cells, such as our peptide–bismuth bicycles, is uncharted scientific territory. As such, it is difficult to predict the effect bismuth may have on cell viability. We selected compounds **1**-**6** and **12**-**14** as representative subsets of the investigated CPPs and conducted cytotoxicity studies in A549 cells using the sensitive Cell Titer Glo assay. To allow sufficient time for potential toxic effects to manifest, cells were incubated for 24 h. For all tested compounds, the cells demonstrated 80% viability up to a concentration of 10 μM (Figures S4 and S5). For model compound **1**, we observed 80% cell viability even at 50 μM, while other peptides significantly reduced the cell viability at higher concentrations. Considering the potential cytotoxicity of polycationic CPPs, it remains uncertain whether bismuth itself contributes to any cytotoxic effects, even at high concentrations. The comparison of cytotoxicity profiles between the control peptides **3** and **5** (Figure S4) and their bismuth analogues **4** and **6** (Figure S5) indicates that bismuth does not have any additional impact on cellular toxicity.

Lastly, we examined the influence of bismuth–bicycle formation on the efficiency of cellular uptake. We investigated two sets of peptides: linear peptides **3** and **5**, and their corresponding bicyclic counterparts, peptides **4** and **6** (Table 1). To ensure a fair and direct comparison between linear and bicyclic peptides, we replaced the cysteine residues in peptides **4** and **6** with serine residues in peptides **3** and **5**, preventing the formation of cyclic disulfides and avoiding the need for potentially cytotoxic concentrations of reducing agent (Figure 2a). For both pairs of CPPs, our time- and concentration-dependent flow cytometry measurements clearly demonstrate that the bicycles exhibit more than one order of magnitude higher cellular uptake than the corresponding linear peptides (Figure 2b/c). This observation is strongly supported by live-cell confocal microscopy experiments, which were conducted in a time- (Figures 2d/e, S18, S19) and concentration-dependent manner (Figures S8–S11).

In conclusion, we have developed the first bismuth-containing peptides that enter human cell lines. These cell-penetrating peptide–bismuth bicycles exhibit efficient cellular uptake at concentrations as low as 10 nM, while also demonstrating no cytotoxic effects at concentrations up to 10 μM. Furthermore, our CPPs have proven effective in delivering cargos such as fluorescent dyes into cells. We demonstrate that the incorporation of three positive charges is sufficient to achieve excellent cellular uptake, and further show that bicyclization significantly enhances the uptake compared to linear peptides. Custom-synthesized peptides can be easily converted into

peptide–bismuth bicycles, and their cellular uptake can be measured using label-free ICP-MS analysis. Our findings open possibilities for future applications in the development of cell-penetrating proteins and the design of bismuth-containing therapeutics.

Acknowledgements

We thank the Australian Research Council for funding support, including a Discovery Project (DP230100079) and Future Fellowship (FT220100010) awarded to CN, as well as a Centre of Excellence (CE200100012) awarded to EJN. JR thanks the Deutsche Forschungsgemeinschaft (DFG, German Research Foundation) – Project-ID 387284271 – SFB 1349 and the DFG-funded core facility BioSupraMol. We thank Prof. Burkhard Kleuser for access to FACS facilities. We appreciate technical support form Dr. Christian Gerecke (FACS), Elisa Quaas (confocal microscopy), and Dr. Nicholas Proschogo (ICP-MS).

Keywords: Peptides • cells • bismuth • bicycles • fluorescence

[1] a) D. M. Copolovici, K. Langel, E. Eriste, U. Langel, *ACS Nano* **2014**, *8*, 1972-1994; b) G. Guidotti, L. Brambilla, D. Rossi, *Trends Pharmacol. Sci.* **2017**, *38*, 406-424; c) P. G. Dougherty, A. Sahni, D. Pei, *Chem. Rev.* **2019**, *119*, 10241-10287; d) M. Richter, A. Chakrabarti, I. R. Ruttekolk, B. Wiesner, M. Beyermann, R. Brock, J. Rademann, *Chem. Eur. J.* **2012**, *18*, 16708-16715; e) M. Barth, R. Fischer, R. Brock, J. Rademann, *Angew. Chem. Int. Ed.* **2005**, *44*, 1560-1563.

[2] S. Wang, Z. Li, D. Aispuro, N. Guevara, J. Van Valkenburgh, B. Chen, X. Zhou, M. N. McCarroll, F. Ji, X. Cong, P. Sarkar, R. Chaudhuri, Z. Guo, N. P. Perkins, S. Shao, J. K. Sello, K. Chen, M. Xue, *J. Am. Chem. Soc.* **2022**, *144*, 20288-20297.

[3] a) A. D. de Araujo, H. N. Hoang, J. Lim, J. Y. W. Mak, D. P. Fairlie, *Angew. Chem. Int. Ed.* **2022**, *61*, e202203995; b) G. Lattig-Tunnemann, M. Prinz, D. Hoffmann, J. Behlke, C. Palm-Apergi, I. Morano, H. D. Herce, M. C. Cardoso, *Nat. Commun.* **2011**, *2*, 453; c) A. F. L. Schneider, M. Kithil, M. C. Cardoso, M. Lehmann, C. P. R. Hackenberger, *Nat. Chem.* **2021**, *13*, 530-539; d) O. Tietz, F. Cortezon-Tamarit, R. Chalk, S. Able, K. A. Vallis, *Nat. Chem.* **2022**, *14*, 284-293.

[4] a) S. Chen, D. Bertoldo, A. Angelini, F. Pojer, C. Heinis, *Angew. Chem. Int. Ed.* **2014**, *53*, 1602-1606; b) C. Heinis, T. Rutherford, S. Freund, G. Winter, *Nat. Chem. Biol.* **2009**, *5*, 502-507; c) S. S. Kale, C. Villequey, X. D. Kong, A. Zorzi, K. Deyle, C. Heinis, *Nat. Chem.* **2018**, *10*, 715-723; d) C. A. Rhodes, D. Pei, *Chem. Eur. J.* **2017**, *23*, 12690-12703; e) S. Ullrich, J. George, A. E. Coram, R. Morewood, C. Nitsche, *Angew. Chem. Int. Ed.* **2022**, *61*, e202208400.

[5] a) W. Lian, B. Jiang, Z. Qian, D. Pei, *J. Am. Chem. Soc.* **2014**, *136*, 9830-9833; b) C. A. Rhodes, P. G. Dougherty, J. K. Cooper, Z. Qian, S. Lindert, Q. E. Wang, D. Pei, *J. Am. Chem. Soc.* **2018**, *140*, 12102-12110.

[6] S. Voss, J. Rademann, C. Nitsche, *Angew. Chem. Int. Ed.* **2022**, *61*, e202113857.

[7] a) P. Gobbo, P. Gunawardene, W. Luo, M. S. Workentin, *Synlett* **2015**, *26*, 1169-1174; b) B. Schroeder, P. Demirel, C. Fischer, E. Masri, S. Kallis, L. Redl, T. Rudolf, S. Bergemann, C. Arkona, C. Nitsche, R. Bartenschlager, J. Rademann, *ACS Med. Chem. Lett.* **2021**, *12*, 1955-1961.

[8] H. J. Forman, H. Zhang, A. Rinna, *Mol. Aspects Med.* **2009**, *30*, 1-12.

[9] a) Z. Qian, T. Liu, Y. Y. Liu, R. Briesewitz, A. M. Barrios, S. M. Jhiang, D. Pei, *ACS Chem. Biol.* **2013**, *8*, 423-431; b) Z. Qian, A. Martyna, R. L. Hard, J. Wang, G. Appiah-Kubi, C. Coss, M. A. Phelps, J. S. Rossman, D. Pei, *Biochemistry* **2016**, *55*, 2601-2612.

[10] P. Lönn, A. D. Kacsinta, X.-S. Cui, A. S. Hamil, M. Kaulich, K. Gogoi, S. F. Dowdy, *Sci. Rep.* **2016**, *6*, 32301.

[11] N. Nischan, H. D. Herce, F. Natale, N. Bohlke, N. Budisa, M. C. Cardoso, C. P. R. Hackenberger, *Angew. Chem. Int. Ed.* **2015**, *54*, 1950-1953.

[12] R. Mohan, *Nat. Chem.* **2010**, *2*, 336-336.